Available online at www.sciencedirect.com
ScienceDirect
Scripta Materialia 58 (2008) 910–913
Scripta MATERIALIA
www.elsevier.com/locate/scriptamat

Nickel foams with oxidation-resistant coatings formed by combustion synthesis

O. Smorygo,* V. Mikutski, A. Leonov, A. Marukovich and Y. Vialiuha

Powder Metallurgy Institute, 41 Platonov Street, Minsk 220005, Belarus

Received 10 November 2007; revised 22 December 2007; accepted 7 January 2008
Available online 16 January 2008

A combustible mixture containing aluminum, titania and boron oxide powders was deposited onto the open-cell nickel foam structural elements. Heating the sample ensured formation of a protective coating based on titanium boride and alumina over the nickel foam struts via the combustion synthesis reaction. Oxidation rate of the resultant composite foam was remarkably lower compared to the bare nickel foam, the stress–strain behavior changed and was dependent on the coating thickness, and the original open-cell structure was retained.

Keywords: Foams; Nickel; High-temperature oxidation; Combustion synthesis

Permeable cellular solids (metallic and ceramic foams) as catalyst supports, filters, heat exchangers, etc., have been an object of extensive studies during the last decade because of their unique combination of high porosity, stiffness and permeability [1,2]. Specifically, open-cell foams are considered to be advantageous catalyst supports in some catalytic processes since they ensure low pressure drops under high flow velocities, enhanced heat and mass transport [3–5] and, if the foam is made from a highly conductive material (metal), effective dissipation of the high-intensity heat within relatively small spaces [6].

Fully open and highly permeable cellular structure can be attained through duplicating the structure of the reticulated polyurethane foam followed by heat treatments to burn out the polymer foam and strengthen the structure. For example, electroplating ensures the manufacturing of the nickel-based open-cell foams with the extremely high porosity up to 98%, excellent permeability and uniform pore structure [7]. Nickel foams of various cell size grades ranging from 5 to 70 ppi are available in the market [1]. However, direct application of such foams as catalyst supports is objectionable because of their poor corrosion and oxidation resistance. That is why much attention has been paid recently to the improvement of the high-temperature oxidation resistance of the commercial open-cell nickel foams.

Several teams demonstrated that pack aluminizing or chromizing are effective processes to form the oxidation-resistant protective layer over the nickel foam structural elements or to convert nickel completely into intermetallics or superalloys [8–11]. In another approach [12], the NiCrAl-superalloy-based precursor powder was deposited onto the structural elements of the nickel foam template by electrophoretic deposition. The subsequent high-temperature vacuum sintering was stated to ensure the continuous protective layer via the transient liquid phase sintering. Both approaches retain the pore structure of original foams and improve remarkably their mechanical properties and oxidation resistance but require rather durable and energy-consuming multi-step treatments.

In this paper, we report a simple method to improve the oxidation resistance of the open-cell nickel foams by forming the protective layer via the combustion reaction in the preliminary deposited powder coating.

Combustion processes utilize the heat of strongly exothermic reactions and can result in the formation of a wide range of intermetallic and ceramic materials with outstanding corrosion properties [13,14]. The method can bring many advantages since it is rather fast and does not require energy-consuming heat treatments at elevated temperatures. The combustion reaction described by the following equation was considered as the model process in the research:

$$10/3\,Al + TiO_2 + B_2O_3 \rightarrow TiB_2 + 5/3\,Al_2O_3 + 900\ kJ \quad (1)$$

* Corresponding author. Tel.: +375 17 292 66 39; fax: +375 17 210 05 74; e-mail: olegsmorygo@yahoo.com

1359-6462/$ - see front matter © 2008 Acta Materialia Inc. Published by Elsevier Ltd. All rights reserved.
doi:10.1016/j.scriptamat.2008.01.014

This reactive mixture is attractive for studies since cheap raw powders are used; rather dense reaction product can result from a non-compact precursor powder layer. The above reaction given by Eq. (1) can be ignited by a simple heating a sample in the air atmosphere at temperatures as low as 700–750 °C [15,16]. The objective of this work was to study the protective layer structure and its effect on the high-temperature oxidation rate and mechanical properties of the resultant foams.

The sample preparation procedure was as follows. Open-cell nickel foam plates (100 × 100 × 20 mm) were prepared by electroplating of the 20 ppi reticulated polyurethane foam in the sulfate electrolyte followed by the heat treatment in the dissociated ammonia atmosphere at 1100 °C during 1 h to burn out the polymeric template and sinter the structural elements. The process is described in detail in Ref. [17]. Resultant foams had a density of about 0.30 g cm^{-3}, which corresponded to the porosity of 96.6%. Then the foam plates were cut into ∅30 × 20 mm samples for further treatments.

A reactive mixture was prepared from the titanium oxide powder in the anatase form (sieved, <40 μm fraction), boron oxide powder (sieved, <40 μm fraction) and aluminum powder (average particle size of 15 μm). The powders in the stoichiometric proportion (33.4, 29.0 and 37.6 wt.%, correspondingly) were put into a dispersion medium (50 wt.%) and the suspension was prepared by mixing components in a jar mixer for 4 h. The 30 wt.% solution of the varnish colloxylin (cellulose nitrate with the nitration degree of 12%) in ethyl acetate was used as the dispersion medium. A thin reactive layer was applied over the nickel foam struts by dipping the samples into the suspension and centrifuging off the excess suspension under the 30*g* overload during 1 min. The application procedure was repeated 1–3 times to vary the layer thickness in different samples. Then the samples were dried in an oven at 150 °C for 2 h, heated to 1000 °C in an electric furnace in the air atmosphere with the heating rate of 10 °C min^{-1}, soaked for 5 min and cooled with the furnace. Heating the samples to 700–750 °C is enough to ignite the reactive mixture [15]. Further heating was supposed to complete the transformation of the precursor mixture. In parallel, untemplated TiB_2–Al_2O_3 foam samples were prepared via the combustion synthesis as well. For this, the 20 ppi open-cell polyurethane foam samples (∅30 × 20 mm) were impregnated with the aforementioned suspension, the excess suspension was removed by centrifuging off and the samples were dried. The impregnating–centrifuging–drying series was repeated three times until the sample raw density reached 0.42 g cm^{-3}. Centrifuging, drying and heat treatment regimes were the same as in the case of the nickel foam templated samples. Porosity of final foams was calculated by assuming that the precursor powders transformed completely into TiB_2–Al_2O_3. The calculated theoretical density (rule of mixtures) of the final TiB_2–Al_2O_3 product amounts to 4.12 g cm^{-3} [16]. Average parameters of resultant foams are summarized in Table 1.

In order to define the static oxidation resistance all the samples were soaked in the air atmosphere in an electric furnace during 55 h with periodic thermal excursion to room temperature to measure their weight gain.

Table 1. Characteristics of resultant foams

No.	Composition (wt.%)	Density (g cm^{-3})	Porosity (%)	Strut width (μm)
1	100% Ni	0.30	96.6 ± 0.2	300–320
2	Ni/24% (TiB_2–Al_2O_3)	0.39	94.8 ± 0.3	360–380
3	Ni/39% (TiB_2–Al_2O_3)	0.49	92.8 ± 0.3	400–420
4	Ni/58% (TiB_2–Al_2O_3)	0.71	88.6 ± 0.3	450–550
5	100% (TiB_2–Al_2O_3)	0.42	90.3 ± 0.5	380–420

The weight gain was normalized to the original nickel foam weight (beside the untemplated TiB_2–Al_2O_3 foam). The weight gain rate was characterized by the parabolic rate constant (k_p) that can be calculated from the following equation:

$$(\Delta M/S)^2 = k_p \tau$$

where ΔM is the sample weight gain, S is the sample surface area and τ is duration of the oxidation testing. The foam sample internal surface area S was calculated from the experimental data by assuming that $k_p = 8.6 \times 10^{-11}$ g^2 (cm^4 s)$^{-1}$ for a pure nickel foam [9].

The foam pore structure and the protective coating observations as well as the elemental analysis were performed using CamScan 4 scanning electron microscope equipped with the INCA 350 energy-dispersive X-ray spectrometer. The compressive testing was performed using the Instron 1195 mechanical testing machine with the cross head speed of 0.5 mm min^{-1}.

Adiabatic combustion temperature calculations for the studied reaction based on the Merzhanov's methodology [18] gave 2326 K, which was much higher compared to the nickel melting point (1728 K). Nevertheless, macroscopic shape and dimensions of the foam specimens were stated to be unchanged after the combustion reaction, the open-cell pore structure was retained but the average strut width increased remarkably after the deposition of the TiB_2–Al_2O_3 coating (see Table 1).

Figure 1 demonstrates the fractured foam strut general view (a) and the strut surface morphology (b) after the combustion synthesis of the TiB_2–Al_2O_3 coating. Two separate phases could be clearly identified across the strut: an inner hollow nickel core encased into a TiB_2–Al_2O_3 shell. No evident diffusive layer between the nickel core and the coating was observed but the interface was substantially continuous. The coating exhibited significant residual porosity, which could be referred to the following causes [15,16]: (i) the coating

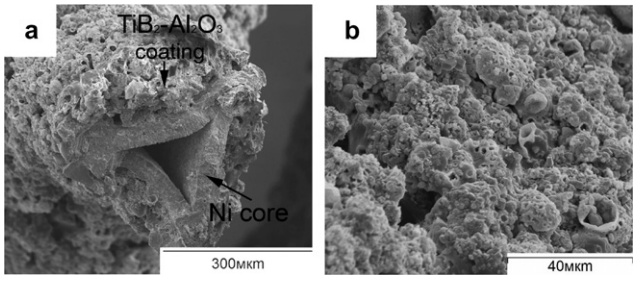

Figure 1. Protective coating morphology: (a) fractured foam strut and (b) coating surface.

undergoes significant volumetric changes during the reaction, the calculated average density (rule of mixtures) increases from ~2.6 g cm^{-3} (original mixture) to ~3.9 g cm^{-3} (final products) and (ii) water absorbed by the moisture-sensitive boron oxide as well as impurities in the technical-grade reactive powders result in the intensive gas release.

Unlike the combustion synthesis of conventional TiB_2–Al_2O_3 products [16], there was no remarkable segregation within the coating neither by porosity nor by composition, which was attributed to the shorter liquid-state duration due to better heat release as well as smaller thickness factor. It should be noted that more complex microstructural analysis, not performed here, would be needed to identify precisely all constituents of the final coating.

Figure 2 demonstrates the mass gain kinetics of the bare nickel foam, Ni–(TiB_2–Al_2O_3) foams with different coating thicknesses and TiB_2–Al_2O_3 foam synthesized without the supportive nickel template. Lines in the figure are the oxidation rate parabolic fits; the corresponding rate constants k_p are given in parentheses. Bare nickel foams exhibited very fast oxidation because: porous NiO surface layer that is foamed in the air atmosphere cannot act as an effective barrier to the oxygen transport. The weight gain rate became apparently slower after the synthesis of the TiB_2–Al_2O_3 protective coating and the thicker coatings ensured better oxidation resistance. As compared to the bare Ni foam, the weight gain rate could be reduced by factor of 3 and k_p approached values reported for the oxidation-resistant Ni–Cr foams [9]. In general, the weight gain in these composite foams could be attributed to two possible mechanisms: (i) oxidation within the protective coating and (ii) oxygen transport through the coating defects resulting in the Ni template oxidation. TiB_2 forming the coating is known to be unstable to the oxidation in air above 800 °C. However, its oxidation is accompanied by generation of the boron anhydride melt, which results in the formation of a diffusion barrier and, furthermore, self-healing of micropores and microcracks [19]. That is why the TiB_2–Al_2O_3 foam samples exhibited the zero-order weight gain. SEM studies did not reveal remarkable morphological changes within the coating of the Ni–(TiB_2–Al_2O_3) foams after the 55 h exposure but a microporous nickel oxide layer formed at the nickel core/coating interface, which resulted in the extensive coating delamination areas. Figure 3 demonstrates the foam strut cross section after the oxidation testing; the nickel oxide area is marked by arrows in the figure. It should be noted that the 55 h exposure did not result in the complete Ni → NiO transformation and unoxidized nickel could be still found in the foam strut core area. The transformation of dense (strong and ductile) nickel to porous (weak and brittle) nickel oxide in the foam strut resulted in the remarkable changes of the foam mechanical properties.

Table 2 summarizes mechanical properties of the studied foams both before and after the oxidation testing. The stress–strain behavior of bare nickel foams was usual of ductile metallic foams: linear elastic deformation at low stresses followed by a long plastic yielding plateau with the slow stress rise and, finally, the steep rise of the stress because of the foam densification with direct contact between cell walls [9]. The yield strength of Ni foam samples was 0.45 MPa. As was expected, nickel foams became very weak and brittle after the testing due to the almost complete oxidation.

In contrast, the stress–strain curves of foams with the protective layer were neither merely ductile nor merely brittle and included two characteristic areas depending on the deformation (Fig. 4). At the initial stage the curve shape was typical of brittle ceramic foams and comprised sequentially: a short initial region of some strut fractures, steep elastic stress increase until the maximum corresponding to the macroscopic crack propagation and the final progressive damage accompanied by the gradual stress drop. It should be noted that, compared to brittle load–displacement plots, the observed ones were much smoother and did not include apparent serrations. At the final deformation stage the curve trans-

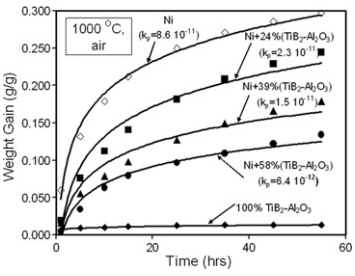

Figure 2. Kinetics of high-temperature oxidation in air of bare nickel, Ni–(TiB_2–Al_2O_3) and TiB_2–Al_2O_3 foams. Oxidation rate parabolic fit constants k_p (gm^2 (cm^4 s)$^{-1}$) are given in parentheses.

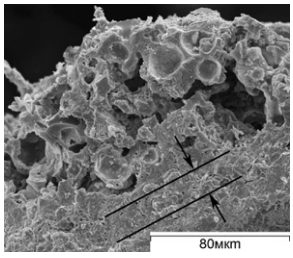

Figure 3. Foam strut/coating interface of the Ni–58% (TiB_2–Al_2O_3) sample after exposure in air at 1000 °C for 50 h.

Table 2. Mechanical properties of resultant foams

No.	Composition (wt.%)	Oxidation at 1000 °C (yes/no)	Compressive fracture stress (MPa)	Yield stress (MPa)
1	100% Ni	No	n/a	0.45
		Yes	< 0.05	n/a
2	Ni/24% (TiB_2–Al_2O_3)	No	0.55	0.27
		Yes	0.82	n/a
3	Ni/39% (TiB_2–Al_2O_3)	No	0.66	0.30
		Yes	0.92	0.11
4	Ni/58% (TiB_2–Al_2O_3)	No	0.69	0.37
		Yes	1.07	0.21
5	100% TiB_2–Al_2O_3	No	0.21	n/a
		Yes	0.29	n/a

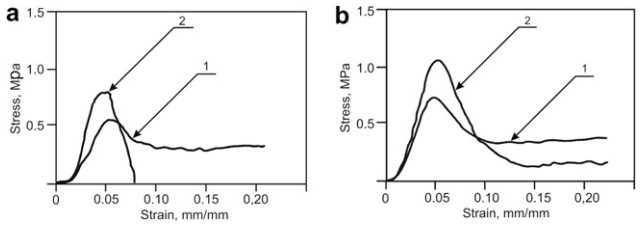

Figure 4. Compressive stress–strain curves of: (a) Ni–24% (TiB_2–Al_2O_3); (b) Ni–58% (TiB_2–Al_2O_3) (b) foams. Curves (1) and (2) correspond to the testing before and after the oxidation testing simultaneously.

formed to the ductile one with the characteristic yielding plateau. In general, the load-bearing ability of the composite foams increased by 80–140% as compared to the bare nickel foam. The yielding stress, however, decreased by 20–40%, which must result from the nickel oxidation during the coating combustion synthesis in the oxidizing atmosphere.

Measurements after the exposure in air at 1000 °C during 55 h indicated noticeable change of the stress–strain behavior. Thinner protective coatings could not prevent remarkable oxidation of the nickel template and the yielding plateau was not observed: the stress–strain curve transformed into the fully brittle one (Fig. 4a). However, the compressive fracture stress increased, which was attributed to the protective coating microcracks healing. In the case of thicker protective coatings the yielding plateau could be still observed after the testing but the yield stress decreased (Fig. 4b) and the compressive fracture stress increased as well.

TiB_2–Al_2O_3 foams that were synthesized without the supportive nickel template, both as-received and oxidized, were weak and crumbled at very low external loads because of a too defective structure.

In summary, combustion synthesis of the oxidation resistant protective coatings is a simple and fast method to improve mechanical and oxidation properties of conventional open-cell nickel foams. The studied composite foams retained original cellular structure while the weight gain due to the high-temperature oxidation decreased remarkably and the overall strength increased. The foam strut structure represented the ductile metallic core encapsulated into the brittle ceramic shell, which affected the stress–strain behavior. The method can be extended to other open-cell metallic foams and other combustible mixtures.

[1] J. Banhart, Prog. Mater. Sci. 46 (2001) 559–632.
[2] L. Montanaro, Y. Jorand, G. Fantozzi, A. Negroa, J. Eur. Ceram. Soc. 18 (1998) 1339–1350.
[3] J.T. Richardson, Y. Peng, D. Remue, Appl. Catal. A – Gen. 204 (2000) 19–32.
[4] Y. Peng, J.T. Richardson, Appl. Catal. A – Gen. 266 (2004) 235–244.
[5] A.N. Leonov, O.L. Smorygo, A.N. Romashko, M.M. Dechko, A.A. Ketov, L.A. Novikov, V.S. Tankovich, Kinet. Catal. 39 (1998) 691–700.
[6] J. Tian, T. Kim, T.J. Lu, H.P. Hodson, D.T. Queheillalt, D.J. Sypeck, H.N.G. Wadley, Int. J. Heat Mass Trans. 47 (2004) 3171–3186.
[7] A.N. Leonov, O.L. Smorygo, V.K. Sheleg, React. Kinet. Catal. Lett. 60 (1997) 259–267.
[8] A.M. Hodge, D.C. Dunand, Intermetallics 9 (2001) 581–589.
[9] H. Choe, D.C. Dunand, Mat. Sci. Eng. A – Struct. 384 (2004) 184–193.
[10] H. Choe, D.C. Dunand, Acta Mater. 52 (2004) 1283–1295.
[11] A. Leonov, A. Romashko, in: J. Banhart (Ed.), Cellular Metals: Manufacture, Properties, Applications, Verl. MIT Publ., Berlin, 2003, pp. 271–274.
[12] L. Yang, X. Wu, D. Weng, Scripta Mater. 55 (2006) 107–110.
[13] A.G. Merzhanov, Ceram. Int. 21 (1995) 371–379.
[14] J. Moore, H.J. Feng, Prog. Mater. Sci. 39 (1995) 243–273.
[15] R.H. Plovnick, E.A. Richards, Mater. Res. Bull. 36 (2001) 1487–1493.
[16] M.A. Meyers, E.A. Olevsky, J. Ma, M. Jamet, Mat. Sci. Eng. A – Struct. 311 (2001) 83–99.
[17] A. Leonov, A. Romashko, in: J. Banhart (Ed.), Cellular Metals: Manufacture, Properties, Applications, Verl. MIT Publ., Berlin, 2003, pp. 158–161.
[18] N.P. Novikov, I.P. Borovinskaya, A.G. Merzhanov, Thermodynamic analysis of self-propagating high-temperature synthesis, in: A.G. Merzhanov (Ed.), Combustion Processes in Chemical Technology and Metallurgy, Institue of Chemical Physics, Chernogolovka, Russia, 1975, pp. 174–187.
[19] G.V. Samsonov, T.I. Serebriakova, V.A. Neronov, Borides, Atomizdat, Moscow, 1975.